Natural Hazards (2025) 121:3099–3122
https://doi.org/10.1007/s11069-024-06921-6

ORIGINAL PAPER

Deformed archaeological remains at *Lilybaeum* in Western Sicily (southern Italy): possible ground signatures of a missed large earthquake

G. Barreca[1,2,4] · F. Pepe[3] · A. Sulli[3] · G. Morreale[1] · S. Gambino[1] · M. Gasparo Morticelli[3] · S. Grassi[1] · C. Monaco[1,2,4] · S. Imposa[1]

Received: 19 December 2023 / Accepted: 11 September 2024 / Published online: 23 September 2024

Abstract
Archaeoseismic analysis performed in Western Sicily points to deformed archeological remains at *Lilybaeum*, a Punic coastal city founded in 397 B.C. at the Island's westernmost edge. Starting from the direct observation of deformed ruins, an interdisciplinary work strategy, which included field-structural analysis, drone-shot high-resolution aerial photogrammetry, and geophysical prospecting, was employed to investigate whether the identified deformations may represent the ground effects of a previously unknown large earthquake in the area. Among the unearthed remains, some mosaics and a stone-paved monumental avenue show evidence of tectonic deformation, being fractured, folded, and uplifted. The trend of folding and fracturing is consistent with the NNW–SSE oriented tectonic max stress axis to which Western Sicily is currently subjected. Displacement along a fracture deforming the *Decumanus Maximus* together with the finding of a domino-type directional collapse, enable us to interpret the observed deformation as the ground signature of a coseismic slip. The seismic rupture occurred along a previously unmapped deformation front that fits well within the seismotectonic context of Western Sicily. Measured offset, geophysical prospecting, and age-constraints all suggest the possibility that a highly-energetic earthquake nucleated in the area following a coseismic rupture along a NE–SW trending back-verging reverse fault towards the end of the fourth century CE. Since seismic catalogs do not provide evidence of such a large earthquake, this event might represent a missed entry in the historical seismic record. This finding provides constraints to redefine the seismic hazard of Western Sicily, a region where recurrence-time intervals for large earthquakes are still unknown.

Keywords Sicilian Collision Zone · Archaeoseismic analysis · Deformed archeological remains · Active tectonics · Historical earthquakes · Seismic hazard

Extended author information available on the last page of the article

1 Introduction

According to both historical and instrumental seismicity, the Sicilian segment of the Apenninic-Maghrebian collisional system in the central Mediterranean (Fig. 1A) is a seismically active zone that has experienced destructive earthquakes (http://bollettinosismico.rm.ingv.it; CPTI15, see Rovida et al. 2020). Seismic records further evidence that largest earthquakes (e.g., the Messina 1908 and Noto 1693, see Meschis et al. 2020; Barreca et al. 2021; Gambino et al. 2021 and reference therein) have occurred mostly in the easternmost portion of the island. In this region, elastic strain accumulates in the crust and cyclically releases mainly along normal or oblique, right-lateral, regional-scale faults at the SW edge of the Ionian Subduction System (Gutscher et al. 2016; Scarfì et al. 2018; Barreca et al. 2019). Moving westwards, the instrumental earthquake dataset reveals how seismicity becomes more scattered, with events characterized by low-to-moderate magnitude ($1 < M < 5.5$) mainly concentrated along the central-inner portion of the Sicilian Collisional Zone (i.e., in the Caltanissetta Basin and Madonie Mts.), and in the southern Tyrrhenian domain (Pondrelli et al. 2006; Billi et al. 2007). Computed focal solutions indicate that seismic faulting in the eastern side of Sicily is dominated by oblique transtensional kinematics whereas central-western Sicily is mostly characterized by nodal planes with reverse-oblique solutions (Scarfì et al. 2021). The pattern of recorded seismicity and related kinematics reflects the current geodynamic scenario where continent–continent (to the west) and continent-ocean (to the east) convergence dynamics take place simultaneously (Barreca et al. 2016). Accordingly, upper plate sectors push against a laterally variable foreland domain, which is characterized by thin descending oceanic crust to the East

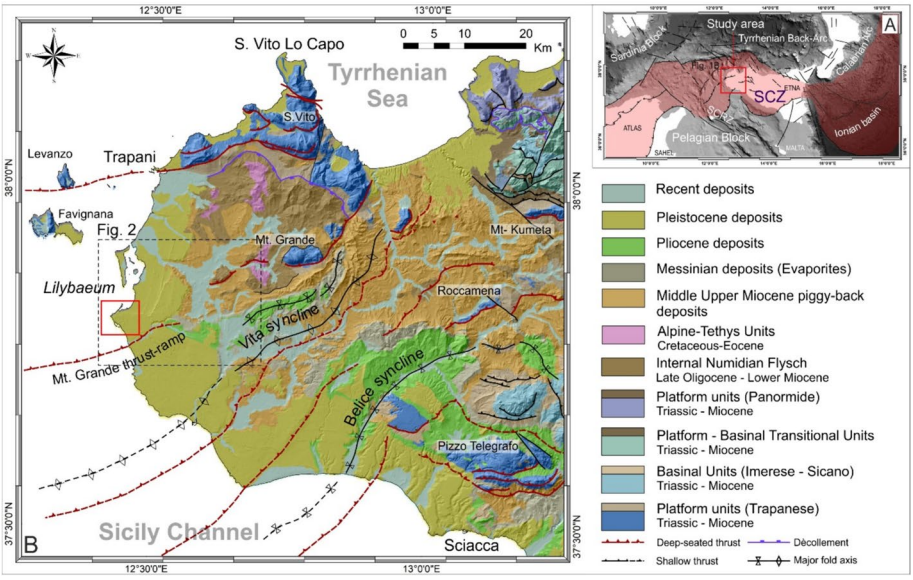

Fig. 1 **A** The study area in the framework of Central Mediterranean tectonics, where the Sicilian Collison Zone (SCZ) is part of the larger suture zone (red light polygon) resulting from the collision between the African and European Plates. **B** Tectonic sketch-map of Western Sicily showing the outcropping stratigraphic series (modified from Lentini and Carbone 2014) and the main tectonic features (shallow and deep-seated thrusts) deforming the region (see also Catalano et al. 2002). The ancient settlement of *Lilybaeum* is located at the westernmost tip of Sicily Island close to a major NE–SW trending deep-seated thrust ramp

a and thicker continental crust to the West. This configuration results in uneven rates of tectonic convergence; higher around the Ionian Subduction Zone (ISZ), and lower in the almost-locked Sicilian Collisional Zone (SCZ). While instrumental datasets provide elements for depicting a consistent seismotectonic picture for the SCZ, the illuminated time-window is limited to the last half-century. This temporal limitation makes it challenging to perform a comprehensive seismic hazard analysis. Pre-instrumental seismic catalogues can help overcome this limitation, providing valuable datasets to evaluate the recurrence time-interval of large earthquakes even if the historical records gradually disappear further back in time. For instance, available historical and parametric catalogs for the Italian territory report earthquakes that have occurred over a long time span (461 B.C.–A.D. 2020, see Boschi et al. 2000; Guidoboni et al. 2019; Rovida et al. 2020). However, data on the effects of historical earthquakes prior to the thirteenth-to fourteenth-century are generally sparse and mostly unconstrained.

Recently, structurally damaged ancient buildings, directional collapses and/or faulted archeological relics have been considered potential indicators of past and missed earthquakes in many tectonically active countries worldwide, provided that other natural and anthropogenic effects are ruled out (Stiros 1996, 2001; Galadini and Galli 1999; Galli and Galadini 2001). In this context, countries rich in ancient ruins and located in seismically unstable areas such as those around the Mediterranean Basin, can be valuable for retrieving additional information to identify possible missed earthquakes from the past. This helps to fill gaps in the historical seismic records. Along the SCZ, the largest amount of archaeological data encompasses the period between the 4th B.C. and the 4th–fifth century CE. This extensive and well-dated archeological substrate has been used to identify previously unknown seismic events (e.g., Guidoboni et al. 2002; Barreca et al. 2014) and to better relocate the source region of large earthquakes reported in historical chronicles (Barreca et al. 2010a).

In this paper, we report on folded-to-displaced archeological relics from the *Lilybaeum* archeological site, a former Punics to Roman settlement located in Western Sicily. Starting from the direct observation of deformed ruins, an interdisciplinary approach has been followed to determine whether the recognized deformation may represent the ground effects of a previously unknown large earthquake in the area. Field structural investigations supported by the analysis of high-resolution, drone-shot photogrammetry and derived digital surface modeling (DSM), along with geophysical prospecting both on land and offshore, all support a tectonic origin of the deformation. According to the amount of dislocation measured along well-dated archeological features and age-constrained directional collapses, a back-verging reverse fault ruptured in the area around the end of the fourth century CE, producing a highly-energetic earthquake. This finding may aid in redefining the seismic hazard of Western Sicily, a low-deforming region where recurrence-time intervals for large earthquakes are longer than instrumental records and, therefore, still largely unknown.

2 Geological background

Western Sicily is a segment of the SCZ (Fig. 1A), characterized by a complex stack of double-verging thrust sheets with NE–SW direction, formed as result of the Neogene-Quaternary Africa-Europe subduction/collisional dynamics (Dewey et al. 1989; Roure et al. 1990; Faccenna et al. 2001a, 2004; Henriquet et al. 2020). In this subduction/collisional framework, tectonic shortening initially involved the Paleogenic deep-water covers of the

subducting Neotethys oceanic domain, creating a large accretionary wedge in response to sediment scraping at the top of the descending oceanic slab (Alpine-Tethys Units in Fig. 1B, see Ogniben 1960; Monaco and Tortorici 1995). During the Oligo-Miocene, portions of the wedge were pushed by the advancing European backstop and progressively transported southward eventually overriding the platform/basin pre-orogenic configuration of the African continental margin (Catalano et al. 1996; Henriquet et al. 2020). As convergence continued, the African paleo-margin was then positively inverted creating a foreland-ward migrating thrust-wedge. This thrust wedge, locally exceeding 20 km in thickness, is formed by deep-water Meso-Cenozoic carbonate units, that override a more than 10 km-thick carbonate platform (Catalano and D'Argenio 1978, 1982; Bello et al. 2000). It is characterized by a multi-stage tectonic evolution during the last 15 My evolving from a thin-skinned to a thick—skinned structural style (Catalano et al. 2013; Gasparo Morticelli et al. 2015; Sulli et al. 2021).The thrust-stack includes Meso-Cenozoic shallow to deep-water carbonate successions (Catalano and D'Argenio 1978, 1982; Bello et al. 2000) deformed into a series of tectonic units bounded by reverse fault contacts. During the tectonic piling, Middle-Upper Miocene terrigenous and evaporitic sediments deposited syn-tectonically in a wedge-top/foredeep migrating system (Gugliota et al. 2014 and reference within). The westernmost segment of the SCZ forms a roughly NE–SW trending contractional belt (Fig. 1B) interposed between two extensional domains, the Tyrrhenian back-arc basin to the north (Faccenna et al. 2001b), and the Sicily Channel Rift Zone to the south (SCRZ in Fig. 1A, see Ben-Avraham et al. 1990). Deep seismic explorations have disclosed many aspects of the crustal setting of Western Sicily, revealing a complex tectonic belt composed of multiple horses that formed at different times and structural levels. (Catalano et al. 2000; Finetti et al. 2005). During the thin-skinned tectonic, two main shallow to deep-seated shortening events affected the Meso-cenozoic carbonate units (see Avellone et al. 2010) creating two superposed structural levels separated by a regional décollement. This major structural discontinuity has been documented on seismic reflection profiles as part of a geometric configuration resembling a duplex deformation context (Catalano et al. 2000; Tortorici et al. 2001; Albanese and Sulli 2012). The upper structural level of the duplex system comprises an early Miocene, 1–3 km-thick system of horses involving both shallow and deep-water terrains (Panormide and Imerese-Sicano units) in a shallow-seated tectonic event. This shallow tectonic wedge is detached at depth along a regional sole thrust over which the entire imbricate fan has migrated southward, slipping over the top layer of the under-thrusting northernmost part of the Pelagian Block (Fig. 1A). Since the late Miocene-Early Pliocene, back-arc opening of the Tyrrhenian domain in the north, along with the cessation of subduction has resulted in continent–continent collision dynamics along much of the SCZ (Bianchi et al. 1987; Bello et al. 2000; Catalano et al. 2013; Finetti et al. 2005; Barreca et al. 2020b). In Western Sicily, this later and still ongoing tectonic stage (deep-seated tectonic event, see Sect. 2.1) has been characterized by the deepening of décollement levels and the formation of foreland-verging horses bounded by deep-seated, high-angle thrust-faults. Overall, thrust contacts and associated wide-wavelength folding have formed a ~ 10 km-thick hinterland-dipping thrust-stack (Catalano et al. 2000; Avellone et al. 2010; Barreca et al. 2010b; Barreca and Maesano 2012). High-angle thrust contacts have remained mostly buried along the eastern portion of the SCZ (Bello et al. 2000; Finetti et al. 2005; Catalano et al. 2013) whereas in Western Sicily, this young thrust system has breached and refolded the previously stacked tectonic units (e.g., the overlaying early Miocene shallow thrust-wedge, see Avellone et al. 2010; Gasparo Morticelli et al. 2017) piercing the topographic surface with large ramp-anticline culminations. Along these structural culminations, the previously under-thrusted foreland succession

have been significantly uplifted and exposed in outcrop (e.g., the Trapani-S. Vito lo Capo Mountains and the Mt. Kumeta–Rocca Busambra ridges to the north and the Mt. Magaggiaro—Pizzo Telegrafo ramp anticline system southward (see Tortorici et al. 2001; Albanese and Sulli 2012; Balestra et al. 2019; Gasparo Morticelli et al. 2017 and Fig. 1B for location).

Since the upper Pliocene, the thrust wedge system has grown through N-verging structures, correlated at depth with the thick-skinned tectonic event, which involves the crystalline basement in the internal sector of the chain (Accaino et al. 2011; Catalano et al. 2013; Gasparo Morticelli et al. 2015). Field investigations and seismic data from the adjacent marine domain have documented broad, active N-verging thrusting throughout the central-western sector of the SCZ (Sulli et al. 2021). According to the Authors, these tectonic features developed in the late collisional stage of the SCZ and are interpreted as the crustal expression of a change in subduction polarity (from N-dipping to S-dipping) occurred in the southern Tyrrhenian margin since the late Pleistocene (see also Billi et al. 2011). The investigated archaeological site is therefore framed within this active contractional tectonic domain and is located close to the continuation toward the southwest of Mt. Grande thrust-ramp (see Catalano et al. 2000, 2002 and Fig. 1B for location). At a more detailed scale, the coastal site of *Lilybaeum* lies on a 20–50 m-thick Early-Middle Pleistocene succession of bioclastic grainstones characterized by a relatively flat topographic morphology (D'Angelo and Vernuccio 1992; Catalano et al. 2017).

According to D'Angelo and Vernuccio (1992), the area of Marsala has been deformed by contractional features consisting of NE–SW trending and S-verging folds and thrusts with associated back-thrusts mapped just to the East of the investigated area (Fig. 2).

2.1 Seismotectonics

Marine terraces mapped along the coastal domain (Ferranti et al. 2021) and regional (Ferranti et al. 2008) to local GPS measurements (Barreca et al. 2020b; Pipitone et al. 2020; Parrino et al. 2022) indicate that Western Sicily has experienced low-strain-rate shortening since at least the Middle Late Pleistocene. These data indirectly suggest a long recurrence time-interval for large earthquakes in the area. Historical catalogs (e.g., Rovida et al. 2020), show that only a few low-to-moderate intensity earthquakes

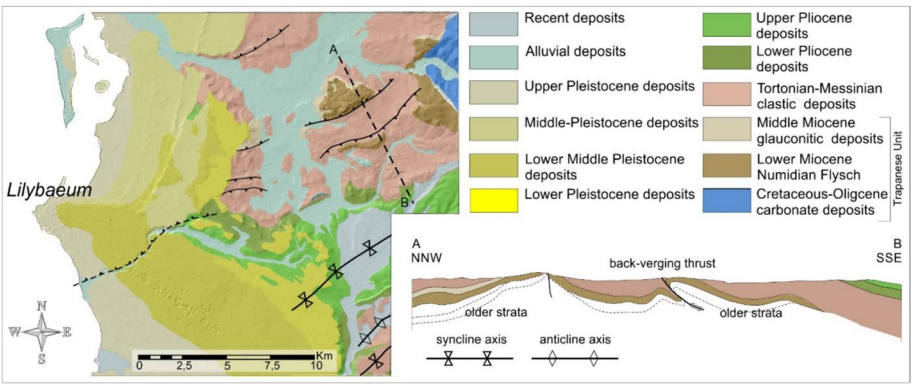

Fig. 2 Detailed geological map of Marsala area and (not in scale) cross-section showing the subsurface structural architecture (modified from D'Angelo and Vernuccio 1992)

have occurred in Western Sicily in the last centuries with no record existing before the XVIII century. Among these, the most energetic earthquake was an I_{max} 7 MCS (Mw = 5.1) event occurred on May 18, 1828. Although its location has remained largely unconstrained, it was located close to the city of Marsala (Molin et al. 2008, and Fig. 3 for location). In January 1968, a seismic sequence with a mainshock of approximately M≃6 struck the Belice Valley in the central sector of Western Sicily, highlighting the seismogenic potential of this part of the Island. Computed focal solutions (McKenzie 1972; Anderson and Jackson 1987) suggest that seismotectonic processes in Western Sicily accommodate active compression at the front of the SCZ. Moreover, the distribution of hypocenters (up to 35 km depth, see Anderson and Jackson 1987; DISS Working Group 2021) indicates that seismic ruptures nucleated along the younger and deeper thrust planes (see Sect. 2 and Monaco et al. 1996; Lavecchia et al. 2007; Visini et al. 2010; Sgroi et al. 2012; Ferranti et al. 2019). Following the 1968 seismic swarm, other earthquakes with M < 5 occurred in Western Sicily such as the seismic shock on June 7, 1981 (Mw = 4.9) (Pondrelli et al. 2006). The seismic event was localized near the city of Mazara del Vallo (see Fig. 3), approximately

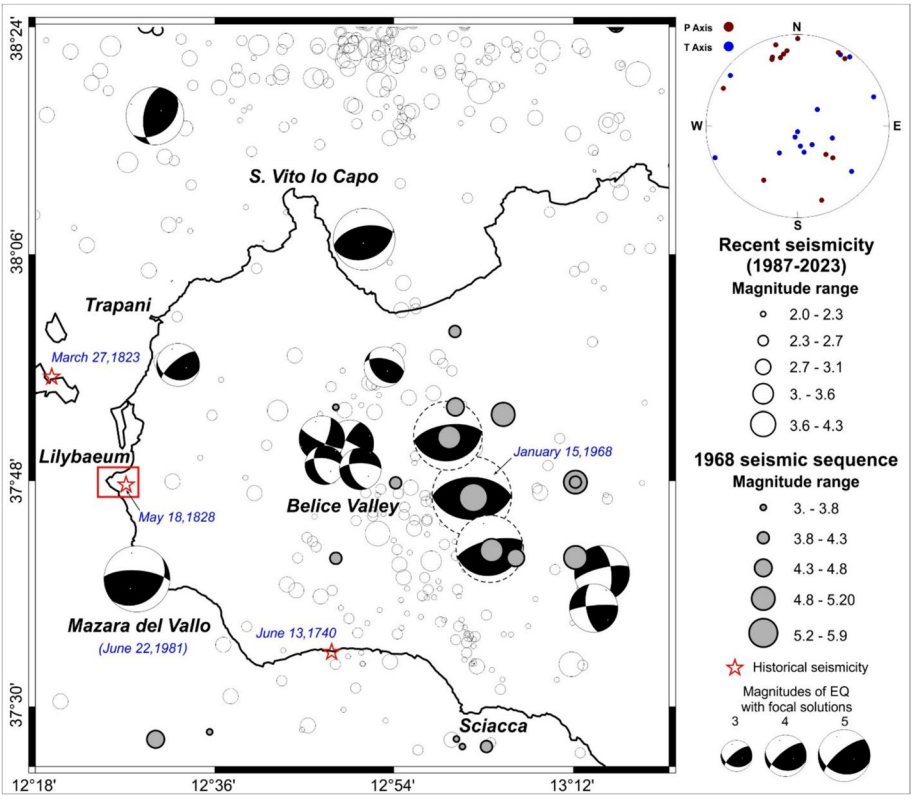

Fig. 3 Seismological map of Western Sicily showing the distribution of historical (red stars) and recent (hollow circles) seismicity (Rovida et al. 2020; INGV-ISIDe). Solid grey circles refer to the 1968 Belice Valley seismic sequence. Focal solutions of recent event with M > 3 (Neri et al. 2005; Alparone et al. 2023) and related P–T axes are also reported. Focal solutions with dashed circles refer to the Belice Valley sequence (McKenzie 1972; Anderson and Jackson 1987)

20 km SE of Marsala (i.e., the investigated site), and nucleated at a depth > 20 km. The seismic rupture exhibited an almost pure reverse mechanism characterized seismic rupture along NE–SW trending nodal planes (Fig. 3). Computed focal solutions of more recent ($M \geq 3$) earthquakes (Neri et al. 2005; Alparone et al. 2023; Courtesy of C. Musumeci), confirm that seismic faulting in the area is mainly characterized by a reverse kinematics resulting from an NNW-SSE trending P-axis (Fig. 3 top-right) consistent with geodetic measurement (Barreca et al. 2014b). According to seismicity recorded over the last 35 years (1987–2023, INGV-ISIDe), only low-to-moderate seismic events ($2 < M < 4.3$) have occurred in Western Sicily during this period. Seismic activity is primarily concentrated in the Belice Valley whit few earthquakes recorded near the site of *Lilybaeum* (Fig. 3).

3 Archaeoseismological analyses

3.1 Methods

Archaeoseismic analysis has been pioneeringly used since the beginning of the last century (e.g., Lanciani 1918; Evans 1928), even if modern and interdisciplinary methodologies have been applied only recently (e.g., Karcz and Kafri 1978; Stiros 1996, 2001; Hancock and Altunel 1997; Noller and Lightfoot 1997; Galadini and Galli 1999; Galli and Galadini 2001). Archaeoseismology aims at identifying pre-instrumental seismic events particularly in regions where damaging earthquakes occur at interval of centuries to millennia (Ambraseys 2006). The study of ancient earthquakes is focused on the identification of specific types of indicators that may be found in the archeological records. These include, among many others, destruction layers, structural damage in man-made constructions, indication of repairs, and abandonments. Where ancient remains are found to be displaced, archaeological features can be exploited as timeline to constrain age and dimension of historical earthquakes. In this view, ground signature (e.g., coseismic deformation) of an earthquake is often maintained for hundreds or thousands of years according to the mechanically hard materials of ancient artefact and the rapid burial they usually undergo.

Methods and limitation in archaeoseismological studies have been firstly provided in Stiros (1996), where typologies of seismic effects on archeological remains are described and classified. Even though discriminating between traces of earthquakes and those of non-seismic origin is rather challenging in archaeoseismological analyses (Ambraseys 2006), the archaeoseismic approach has been successfully applied in many seismically unstable countries to detect and/or infer the occurrence of past earthquakes. From this perspective, countries hosting ancient ruins, such as those bordering the Mediterranean Sea, may represent a potential natural laboratory for these kinds of studies. Many examples of damaged and/or displaced archeological remains come from several places around the Mediterranean basin including Turkey, central Italy and southern Alps (see Galli and Galadini 2001 and reference within), Spain (Rodríguez-Pascua et al. 2023), Calabria (Cinti et al. 2015), and Sicily (Barreca et al. 2010a,b, 2014). In the case here presented, in addition to applying classic archaeoseismic methods, a cross-disciplinary strategy has been followed by combining geological, archaeological, and geophysical investigation that allowed to solve the seismic/non-seismic ambiguity.

3.2 The ancient city of Lilybaeum: chronological markers

The investigated archaeological site is located at the westernmost tip of Sicily Island (southern Italy) and hosts the ruins of the ancient *Lilybaeum*, a coastal city founded by the Punics in 397 B.C. (Di Stefano and Moscati 1993) (Fig. 4A). Extensive archaeological excavations in the area (Giglio 2009; Baumer and Mistretta 2020 and reference within), have uncovered much of the urban setting whereas dating of archeological layers has provided an almost complete chronological evolution of the ancient settlement. According to archeological data, the site was occupied more or less continuously between the fourth century B.C. and the sixth century CE (Mistretta 2016). The presence of numerous luxurious private buildings, with a wealth of featuring thermal baths and polychrome mosaics, suggest prosperity of the city until the 3th century CE (Roman Empire), before it was largely abandoned shortly thereafter (fourth-fifth century CE, Palazzo and Vecchio 2013). Archeological surveys and geophysical prospecting (Giglio 2006), reveal a quadrangular-shaped urban setting characterized by a road network arranged in a regular grid where main roads (*Decumanus or Plateia*) are laterally joined by secondary ones (*Cardines or Stenopoi*). One of the most notable archaeological remains is the *Decumanus Maximus*, a NW–SE oriented stone-paved monumental avenue connecting the harbor to the *civitas* (Giglio 2011, Fig. 4B). As epigraphically attested, the *Decumanus Maximus* was likely paved in late Republican Age (1th century B.C, see Silvestrini 2013). Discovered in 2001 and progressively unearthed up to 2011, the street is today exposed for a total length of 115 m. It exhibits a 5.3 m-wide convex-up track (designed to allow rainwater to run off along the sides), paved with 15–20 cm-thick rectangular blocks of withe limestones and edged on both sides by 0.6 m-wide drainage canals (*opus spicatum*). Between the third and fourth century CE, blocks of calcarenites were placed above the drainage canals to form sidewalls bordering the *Decumanus* along its southern boundary (Palazzo and Vecchio 2013). After the fourth century CE., significant structural transformations affected the

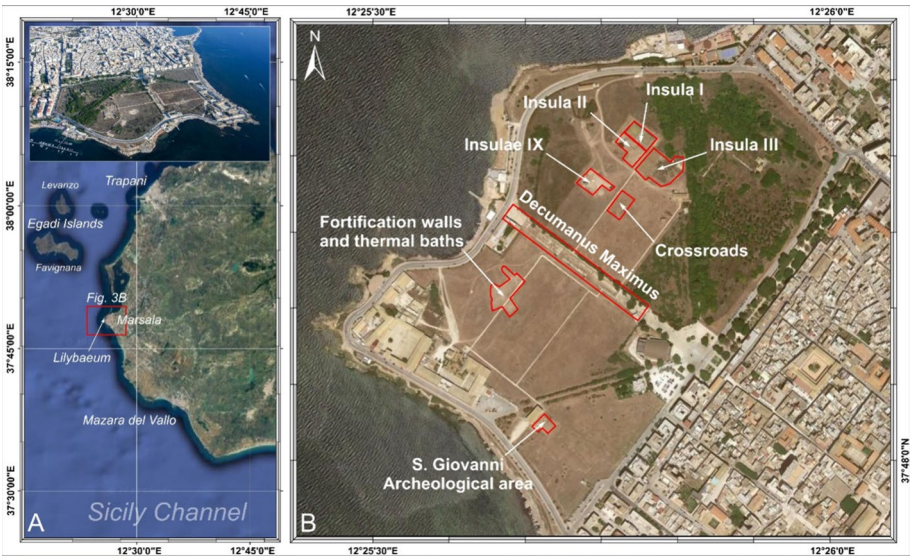

Fig. 4 **A** Location of the ancient settlement of *Lilybaeum* in the geographic frame of Western Sicily. **B** The investigated archaeological site with the major unearthed archaeological remains

areas facing the *Decumanus*. This new arrangement is documented by paved floors, mainly made with recycled materials, built around several kilns alongside the *Decumanus*. Pottery pieces and coins from late 4th-early fifth century CE found in the soil layers overlaying the paved floors predate the structural transformations (Palazzo and Vecchio 2013). From the fifth century CE onward, the first major change in the *Lilybaeum* urban setting occurred marked by abandonments, reuse, and repurposing which also led to the final obliteration of the *Decumanus* as a monumental avenue and its new function as a Byzantine graveyard (Giglio 2011). About the *Cardines*, they were identified to connect with the *Decumanus* both south and north (Palazzo and Vecchio 2013). Here, a spectacular stone-paved cross-road has been unearthed only recently (Mistretta 2022, Fig. 4B).

In the northeast sector of the archeological site, remains of private buildings with multiple rooms and thermal baths, decorated with polychrome mosaics, have been unearthed since the last century. These features, currently well exposed at *Insula I*, are part of the so-called *Roman Domus* (Fig. 4B). According to archeological data, the *Roman Domus* was built between the end of the second and the beginning of the third century CE, following an urban reorganization during which a previous Hellenistic settlement (second century B.C.) was preserved and incorporated in the new one. According to Caruso (2008), *Insula I* was partly destroyed by a violent earthquake probably occurred before the fifth century CE. Following this destruction, the area was converted into a productive district with kilns built directly in the center of some mosaics. All the archeological features described above have been analyzed to detect clues or traces of deformation and exploited as chronological markers.

3.3 Evidence of deformed archeological remains

Direct field observations within the archaeological site, supported by high-resolution aerial photos and accurate profiling over generated digital surface model (DSM), enabled us to identify and characterize the deformation affecting the archaeological remains at several locations. Along its path, the *Decumanus Maximus* (see Fig. 4B for location) shows an unusual NE–SW trending step where blocks of white limestone paving the road are broken and displaced (Fig. 5A). High-resolution profiling over the DSM (inset in Fig. 5A), revealed that the road is displaced by about 10 cm and both blocks siding the fracture are deformed as well. In particular, the raised block (SE-side), is gently folded to create an anticline that has its hinge coaxial to the fracture. Conversely, the lowered block (NW-side) is slightly tilted (~3.5°) approaching the fracture, while a buckled surface characterizes the paving further west (Fig. 5B). A conjugated (Andersonian-type) set of fractures has been observed to pervasively affect the paving in the lowered block (Fig. 5C) along with slightly laterally extruded slabs at the road edges (Fig. 5D). Folding and/or anticorrelation also appear to affect the III–IV century A.D. sidewalls (younger than the paved-road, see Sect. 3.2) on the SW side of the *Decumanus* (Fig. 5E). Even though the displacement affecting the *Decumanus* decreases toward the SW, misalignment of building calcarenite blocks supports the continuation of the deformation even outside the road (Fig. 5F). Moreover, longitudinal tiles-grouts NW of the fracture are out-of-alignment, suggesting either an anticorrelation (caused, for instance, by a ~ 15 cm-lateral offset) or a distortion (Fig. 5G). At the *Insula IX*, about 100 m NE of the *Decumanus* (Fig. 4B), a cross-road was recently discovered by archaeological surveys (see Mistretta 2022). Analysis performed over the drone-shot photogrammetry and high-resolution profiling over the DSM (Fig. 6A and B), revealed that the NE–SW trending *Cardo* is unusually tilted toward the NW by about 3°.

Fig. 5 **A** View from the NW of the stone-paved *Decumanus Maximus* showing the NE–SW trending fracture displacing the road. Inset 1) Forward modeling performed over the restored (horizontal) paved road, predicting that folding (Fig. 5B) and displacement along the *Decumanus* may be attained when about 20 cm of tectonic slip is applied to a reverse fault that dips of 30–35° toward the SE. **B** High-resolution topographic profile (V.E. 8X) over the derived DSM (trace on Fig. 5A top-right) passing through the fracture and showing deformation affecting blocks siding the fracture. **C** Conjugated (Andersonian-type) set of fractures in the lowered, NW block siding the fracture. **D** Laterally extruded slab along the SW edge of the *Decumanus*. **E** Folded 3th-fourth century CE. sidewalls at the SW edge of the *Decumanus*. **F** misalignment of masonry blocks at the prosecution toward SW of the fracture affecting the *Decumanus*. **G** Out-of-alignment (anti-correlation or distortion) of the tiles-grouts NW of the fracture

As pointed out by the altitude/position of the edging stones of the cambered road surfaces, the road section is slightly rotated according to the *Cardo's* longitudinal axis. These results in a lowering (by around 15 cm) from its original position of the NW side of the road, assuming a pivot point at the SE edging stone (Fig. 6B). Evidence of slightly deformed ruins has also been found at the *Insula I* in the NE sector of the investigated archaeological site (see Fig. 4B for location), where floor mosaics from the Hellenistic period (c. second century B.C.) are characterized by rippled to folded surfaces. An asymmetric folding with a hinge-axis aligned approximately N75E deforms the *Cave Canem* (i.e., beware of the dog, Fig. 7A). In this case, high-resolution profiling over the DSM showed that bending and uplifting have affected the SSE block of the mosaic, whereas tilting is observed in the NNW block (Fig. 7B). Adjacent to the "*Cave Canem"*, another mosaic originally paving the *adyterium* (i.e., the dressing room, Fig. 7A) is folded to form a gentle syncline (Fig. 7C). The DSM's contour-mode visualization provides additional insights into the deformation trend, pointing to a coaxiality of contractional features affecting both the mosaics (Fig. 7D).

3.3.1 Origin of deformation

It is worth noting that the NE–SW trends of deformation (fracturing and folding), observed in the examined archaeological remains (*Decumanus*, *Cardo*, and mosaics at *Insula I*), are all consistent with the NNW-SSE oriented tectonic maximum stress axis currently affecting Western Sicily (see Sect. 2.1 and Fig. 3). Furthermore, the uplift-folding on the block SE of the fracture slicing the *Decumanus* (Fig. 5B), and the mosaics at *Insula I* (Fig. 7B) support a tectonic origin for the deformation as the raising of these blocks contrasts with gravity-driven subsidence observed in the lowered blocks. Schepis (2017) adds that there is no evidence of hypogeal cavities or cisterns beneath the analyzed floor mosaics at *Insula I* thus excluding masonry collapse.

Conjugated fractures, slab extrusion, and distorted or misaligned tiles and grouts along the *Decumanus* align with the paved road experiencing compression according to a sub-horizontal maximum stress axis. In this context, the discontinuity transversally offsetting the *Decumanus* may be interpreted as a N40E oriented back-verging reverse fault. Computer-based forward modeling performed over the restored (horizontal) paved road, predicts that the observed folding and displacement occur when about 20 cm of tectonic slip is applied to a reverse fault dipping of 30–35° toward the SE (see inset 1 in Fig. 5A). The thrust-fault appears to not continue southwestwards as indicated by its tip occurring in the paving close to the road edge (Fig. 5F). However, a misalignment in the masonry of calcarenite blocks is observed a few meters further to the SW (Fig. 4F). Considering Romans civil engineering skills in road construction, the tilting affecting the *Cardo* at *Insula IX* (Fig. 6C), appears unusual and suggests that even this structure

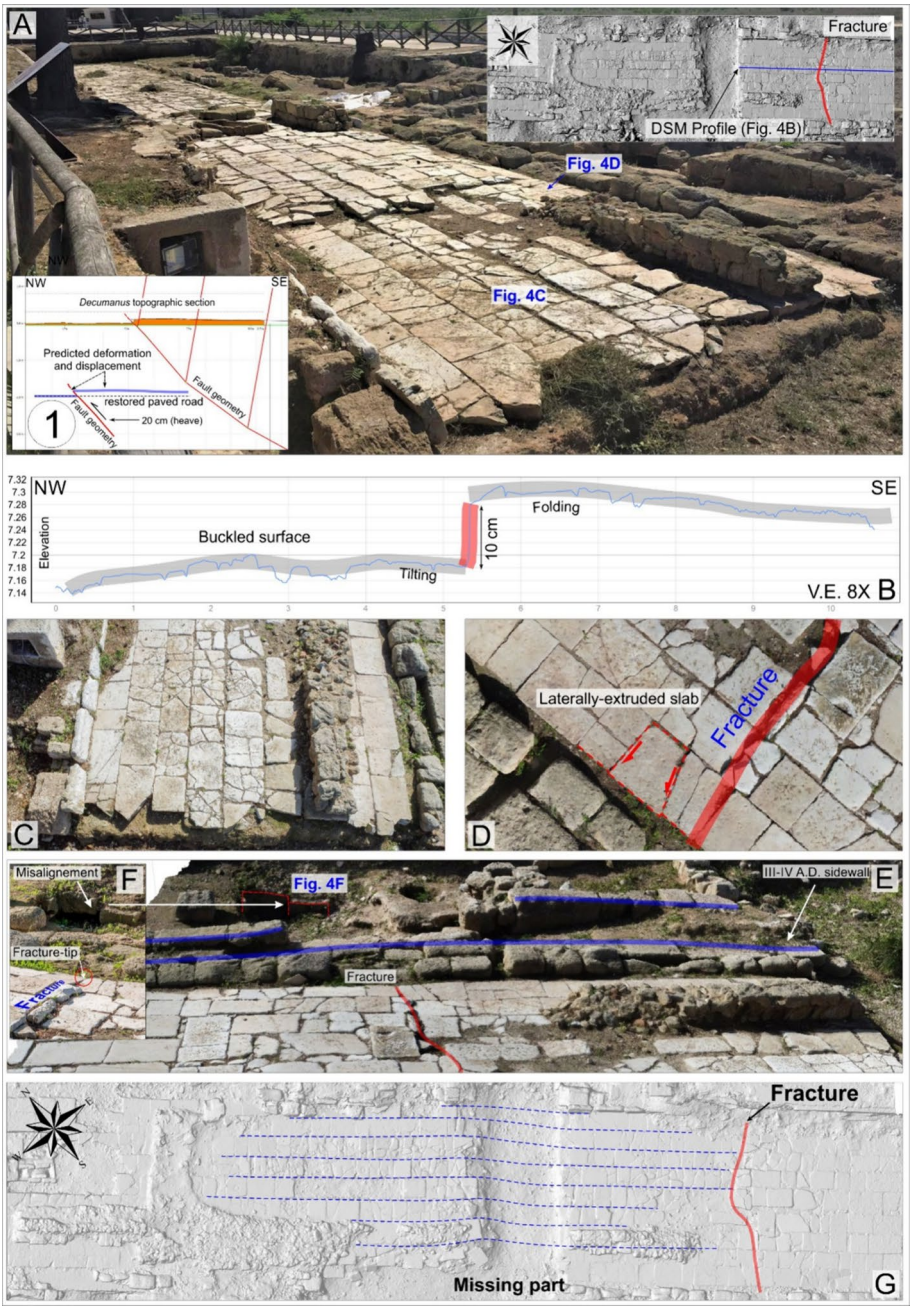

may have been involved in tectonic contraction. Given the orientation of the *Cardo* (NE–SW, see Fig. 6), which is coaxial with the reverse fault displacing the *Decumanus* (see Fig. 5), the measured tilting could be the result of a recent NE–SW trending anticline growing in the area.

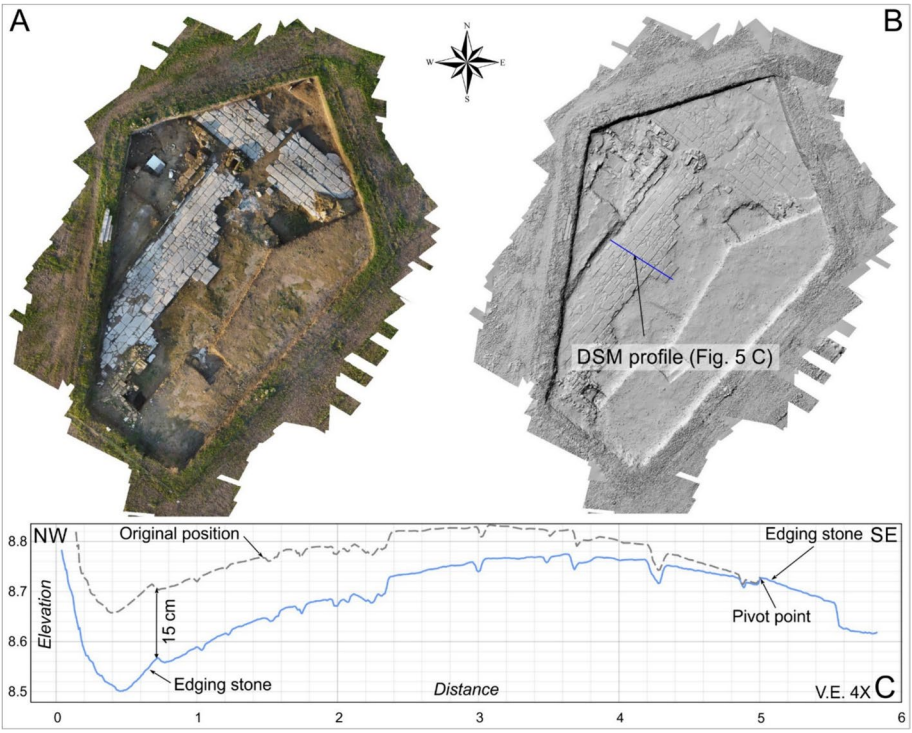

Fig. 6 **A** Drone-shot aerial photograph of a crossroad unearthed at *Insula IX* (see Mistretta 2022) and derived DSM (**B**). **C** High-resolution topographic profiles (light-blue, V.E. 4X) transversal to the NE–SW trending Cardo (trace on **B**) showing a tilting of the road toward NW. The dashed light-gray line is the imaged original position of the road section

4 Geophysical prospections

With the aim of exploring the underground geological setting beneath the *Decumanus Maximus* and search for a possible lateral continuation of the field-observed discontinuities, geophysical surveys were performed both on-land, close to the paved road, and in the near-offshore southwest of the archaeological site.

4.1 On-shore; ERT surveys

A non-invasive electrical resistivity survey was performed near the *Decumanus Maximus* to search for a potential subsurface signature of the field-observed discontinuity (Fig. 8A). The apparent resistivity of rock material with depth was measured using a MAE X612-EM + multichannel georesistivimeter in a Wenner-Schlumberger electrode setup (576 measuring quadripoles). Forty-eight steel electrodes spaced 3 m apart, covering a total length of 140 m, were used for each resistivity deployment (Patti et al. 2021; Imposa et al. 2024). The measured apparent resistivity values, which differ from the real resistivity values (Loke et al. 2003; Imposa et al. 2007; Grassi et al. 2022), were subjected to inversion processes using Res2Dinv software. This software utilizes finite element or finite difference mathematical calculations to obtain 2D resistivity pseudo-sections (ERT,

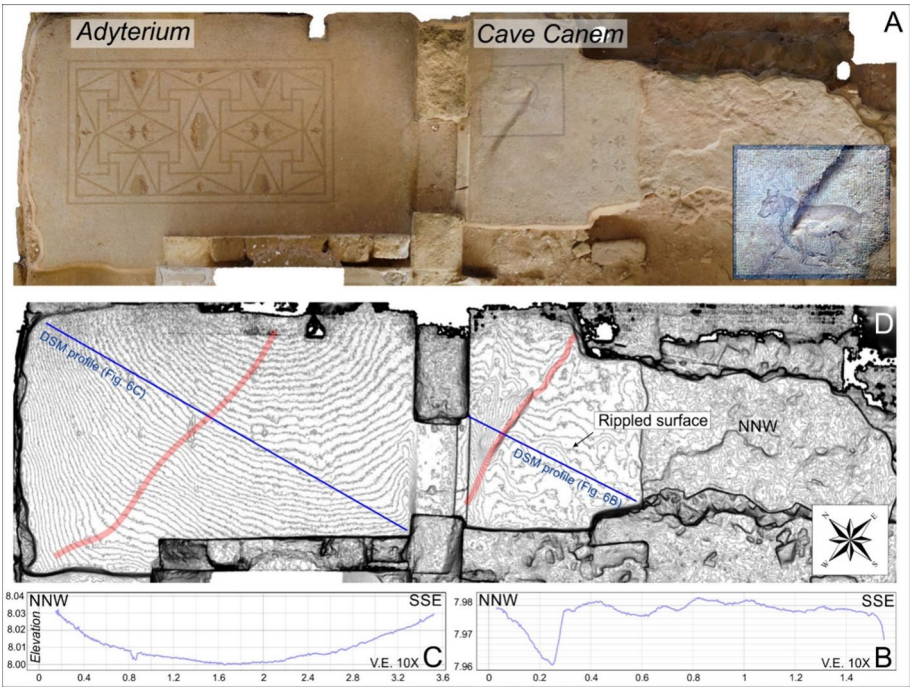

Fig. 7 **A**II century B.C. floor mosaics (*Cave Canem* and *Adyterium*) at *Insula I*. **B**–**C** High-resolution topographic profiles (V.E. 10X) over the derived DSM passing through mosaics (traces on D) showing theyr deformation. **D** DSM's contour-mode visualization of the mosaics showing the rippled surface of the *Cave Canem* and providing additional insights into the deformation trend (light-red lines). Note the co-axiality of contractional features affecting both the mosaics

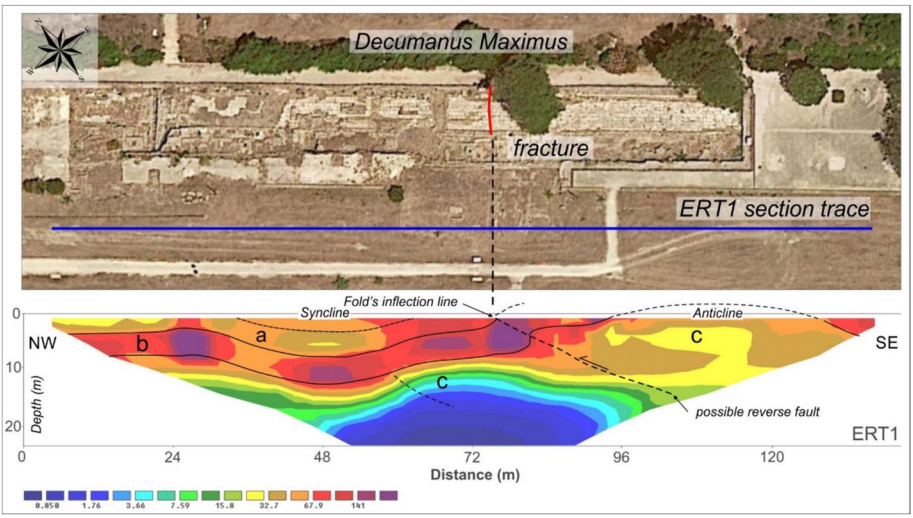

Fig. 8 ERT section acquired parallel to the *Decumanus Maximus* showing the sub-surface setting beneath the road. Interpretation provide insight on the structural pattern affecting the area that appears to be dominated by folding and thrusting

Electrical Resistivity Tomography, Barker 1989). A 2D ERT section, oriented parallel to the *Decumanus Maximus* (NW–SE direction), was then recorded and plotted using a logarithmic color-bar (Fig. 8B). The obtained section illuminates the subsurface setting where primary layers with distinct resistivity values can be detected. The shallowest layer (Unit a in Fig. 8B), appears as a discontinuous low-resistivity unit (20–30 Ω*m). The layer below is characterized by the highest resistivity values ($\rho > 70$ Ω*m) and can be followed for much of the section mainly in the first 10 m of depth (Unit b in Fig. 8B). Two further zones with resistivity values that tend to decline with depth are found below this layer. The shallowest of these has resistivity values in the range of 20–50 Ω*m while the deepest has resistivity values below 4 Ω*m (Unit c in Fig. 8B). Following local surface geology (D'Angelo and Vernuccio 1992; Catalano et al. 2017), the various resistivity layers have been tentatively interpreted as geological units. The low resistivity top-layer is interpreted as upper Pleistocene-Holocene deposits (Catalano et al. 2017). The highly-resistive layer below is associated with Early-Middle Pleistocene grainstones, which are widely exposed in the coastal region surrounding the investigated archaeological site. The intermediate and deepest resistivity layers are interpreted as dry and wet (salty water) arenaceous to sandy-marly clays material (i.e., the Plio-Pleistocene Narbone and Belice formations, see Catalano et al. 2017), respectively. Although the ERT section does not clearly allow for the detection of rock fracturing, it provides information for interpreting the structural pattern of the investigated subsoil domain. The 5–7 m-thick high-resistivity layer (i.e., the Early-Middle Pleistocene grainstones) is found to occur along a significant portion (from 0 to 95 m) of the ERT1 section (Fig. 8B). This high-resistivity unit is clearly folded as indicated by the undulated geometry of its top and bottom boundaries. Toward the SE, the layer is progressively uplifted. This outline resembles a syncline/anticline deformation pattern (Fig. 8B). In this context, the projection of the fracture affecting the *Decumanus Maximus* along the ERT1 section (Fig. 8A), revealed that the discontinuity displacing the stone-paved road roughly align with the ideal projection at the surface of the fold's inflection line (sensu Ramsay 1967), where rock breakthrough is expected. The ERT survey close to the *Decumanus Maximus* confirms that the investigated area is deformed by folds and reverse faults consistent with the ongoing tectonic shortening affecting this region of Western Sicily (see Sect. 2.1).

4.2 Off-shore; sparker surveys

Marine geophysical soundings were performed in the near-offshore sector of the investigated archaeological site to determine whether the deformation front reconstructed on land may extend laterally in its average NE–SW direction. The survey covered a sector of the continental shelf off Marsala and consisted of the acquisition of ten NW–SE trending, tightly-spaced (0.4–0.2 km) high-resolution, single-channel seismic profiles (Fig. 9A). The seismic dataset was acquired using an acoustic source consisting of a Mini-Spark 1000 high-voltage power supply coupled with a Geo-Source 200 multi-tip array fired at 300 ms intervals. Data were recorded with the Geo-Sense Mini Streamer with arrays of 8 elements for 250 ms two-way time (TWT) at a 10 kHz (0.1 ms) sampling rate. The dataset was processed using the Geo-Suite software package and a series of mathematical operators were applied to improve the quality of the seismic signal. The achieved vertical resolution is up to 0.7 m near the seafloor. The seismic and sequence-stratigraphic analysis allowed the identification of three seismic stratigraphic units based on their strata architecture and

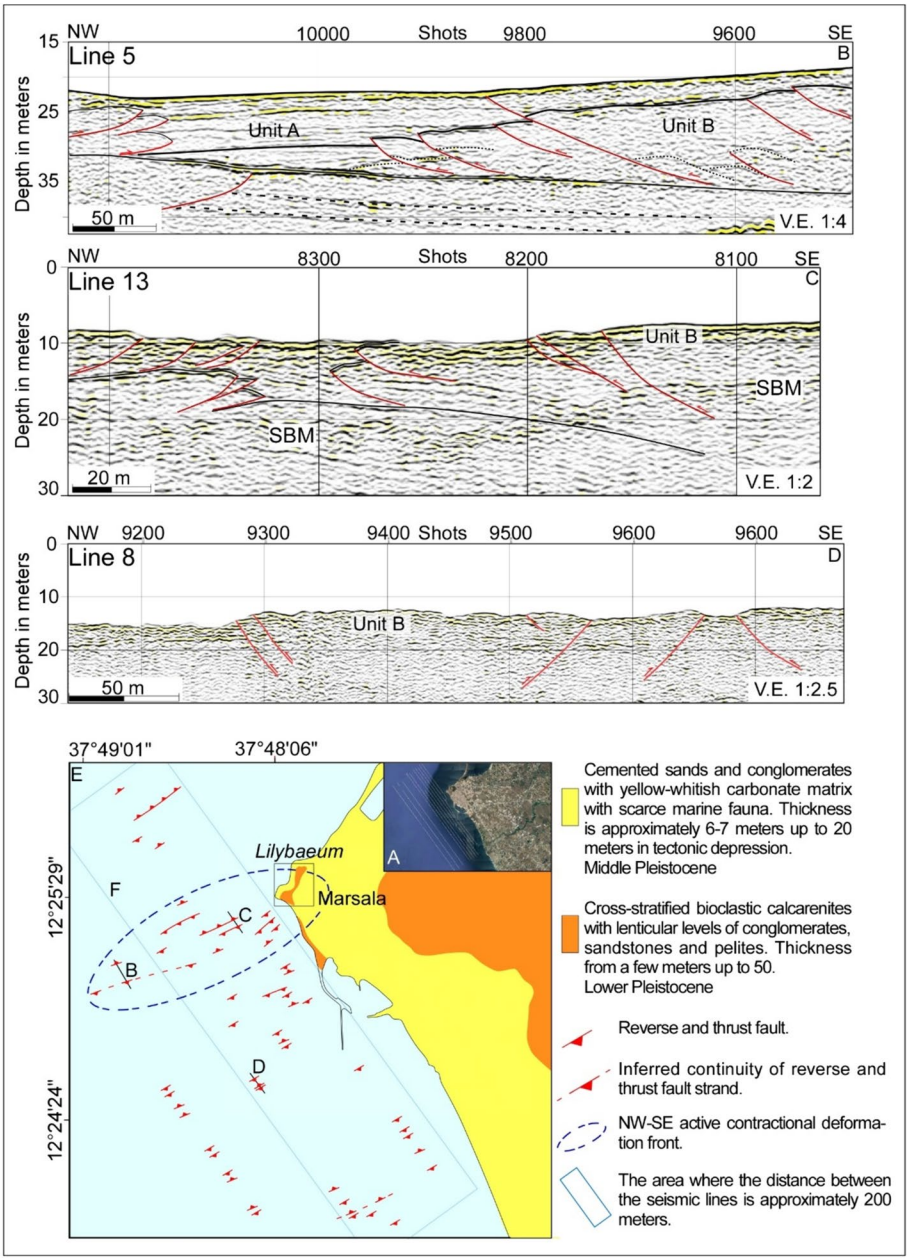

Fig. 9 **A** Inset showing the location of the seismic profiles. **B**–**D** Depth-converted NW-SE high-resolution seismic profiles and their interpretation. Unit A = Upper Pleistocene-Holocene deposits; Unit B = Middle Pleistocene deposits; Unit C = Lower Pleistocene deposits; **E** structural map of the continental shelf offshore Marsala. **F** The area where the distance between the seismic lines is approximately 200 m

seismic characteristics (e.g., amplitude, frequency, and lateral continuity of seismic reflectors). The seismic units were labeled from younger to older as Units A to C (Fig. 9B–D).

Unit A is seismically characterized by layered and parallel, slightly NW dipping configuration, with medium to high-frequency, low-to-medium amplitude reflections (Fig. 9B). The top and base of Unit A correspond to the sea bottom and a high-amplitude reflector. Calibration of Unit A with the stratigraphic succession sampled in the well-logs close to the investigated area (see Ferranti et al. 2019 for details) indicates a correlation with the Upper Pleistocene-Holocene deposits. The maximum thickness of Unit A is about 11 m (~ 1700 m/s).

Unit B is seismically characterized by variable amplitude discontinuous reflections with moderate lateral continuity (Fig. 9B–D). A medium- to high-amplitude, laterally continuous reflector defines its top. Locally, the top of Unit B corresponds to an irregular surface coinciding with the seafloor. We correlate Unit B to the Lower-Middle Pleistocene cemented sand and conglomerates locally topped by bioclastic calcarenites with levels of conglomerates, sandstones and pelites that are widespread along most of the onshore sector of Marsala (Fig. 9E).

Following the seismic facies analysis, the seismic lines were time-to-depth converted using velocity intervals of 1500 and 1700 m/s for the water column and Pleistocene-Holocene sedimentary units, respectively.

All seismic profiles show a series of small-scale bathymetric highs and lows on the seafloor that are generally bounded by reverse and thrust faults, as indicated by according to dislocated reflectors and/or juxtaposition of reflection panels with different seismic characteristics. Reverse and thrust faults have propagated within the Quaternary sedimentary series often dislocating or folding the seafloor. In general, the detected structural features exhibit opposite dipping (toward NW and SE), forming overall small-scale triangle zones (Fig. 9B) and pop-up structures (Fig. 9D). Horizontal and vertical displacement on the thrust faults is generally less than a few tens of meters. Spatial correlation of tectonic structures identified on seismic profiles suggests a strike averaging N60E for most of the reverse faults in line with the roughly NW–SE oriented regional shortening (see Sect. 2.1). Although reverse and thrust faults are widely distributed over the investigated marine sector, shortening appears to be more localized, with a greater concentration of structures in the area extending offshore from the investigated archaeological site (Fig. 9D). Trends of offshore tectonic structures delineate a NW–SE deformation front, is interpreted as the continuation towards the SW of the deformation pattern reconstructed from the deformed ruins within the archaeological site being compatible in location, direction, and kinematics.

5 Discussion

Archaeological evidence for an earthquake is not always clear since other natural and anthropogenic effects may equally lead to deformed architectural relics. Therefore, discriminating between traces of earthquakes and those of non-seismic origin (e.g., landslides, liquefaction, sediment compaction) is crucial in archaeoseismological analyses (Ambraseys 2006). A cross-disciplinary strategy that combines geological, archaeological, and geophysical investigation, can help solving the seismic/non-seismic ambiguity that frequently arises when dealing with damaged ancient remains (Stiros 1996). When the seismic origin of deformation is verified by independent evidence and other factors are ruled

out, damaged, tilted, and displaced ancient remains can provide valuable data for understanding active tectonics and seismic hazards of a region.

The ancient city of *Lilybaeum* was built on an almost-topographically flat coastal area and most of the unearthed man-made structures have their foundations on a thick layer of mechanically hard grainstones (i.e., the Marsala calcarenites, see D'Angelo and Vernuccio 1992; Catalano et al. 2017) or, locally, on indurated cultural debris. In this context, non-seismic causes such as slope instability and sediment compaction cannot be considered the source of the observed deformation given the site's morphology and the stiff lithology of the outcropping rocky series. Even though sinkholes have been reported to form within the Marsala Calcarenites (Catalano et al. 2017), a localized gravity-driven collapse of the bedrock is inconsistent with the against-gravity uplift-folding observed to affect the block SE of the fracture slicing the *Decumanus* (see Sect. 3.3 and Fig. 5B). The contention that (i) folding and tilting affect the blocks separated by the fracture slicing the *Decumanus*, and (ii) the NE–SW trends of deformation characterizing all the analyzed archaeological remains are roughly perpendicular to the NNW–SEE trajectory of the tectonic maximum stress axis that Western Sicily is currently undergoing (see Sect. 2.1 and P-axis in Fig. 3), primarily accounts for a tectonic origin of the deformation. According to Rodríguez-Pascua et al., (2011), most of the deformations observed in the investigated archaeological site can be classified as Earthquake Archaeological Effects (EAEs). These include, among others, conjugated fractures on regular pavements (XFP), and folds on regular pavements (FPV), both of which have been detected in the field along the paving of the *Decumanus* and in the Hellenistic mosaics at *Insula* I (see Fig. 5C and 7B, respectively). The tectonic origin of deformation is also supported by sub-surface geophysical imaging performed on-land and offshore, which provides robust hints regarding the lateral and in-depth continuation of the surface-observed deformations.

As a result, the surface breaks, folding, and tilting that affect the *Lilybaeum* remains as well as the latest seafloor displacement in the offshore, are interpreted as part of a contractional coseismic deformation field produced by the nucleation in the area of an earthquake of considerable dimension. Information about the quake's size may be retrieved by exploiting the amount of dislocation measured along the *Decumanus* (~ 10 cm, Fig. 5B). Following the Displacement-Moment Magnitude regression curve available for reverse faults (Wells and Coppersmith 1994; Leonard 2010), a Magnitude (M) = 6.5 seismic event is obtained assuming the measured offset as an average displacement (AD) along the whole coseismic deformation zone. The analysis of historical cataloges (Rovida et al. 2020), reveals no records of seismic events with the estimated magnitude in Western Sicily. The most energetic quake reported in the cataloges is the I_{max} 7 MCS seismic event (estimated Mw = 5.1, see Sect. 2.1), that occurred on May 18, 1828 close to the city of Marsala (see Fig. 3 for location). Even though the magnitude of this historical earthquake is insufficient to produce the measured ~ 10 cm of displacement, its location indicates a reactivation of the same seismogenic source that likely ruptured in the area several centuries earlier (see Sect. 5.1).

5.1 Dating the seismic event

Once the origin of deformation has been determined, a major challenge in archaeoseismic analyses is to provide constraints on the timing of the coseismic deformation (Stiros 1996). Deformed archaeological remains at *Lilybaeum* span ages from the second century B.C. (i.e., the folded *Cave Canem*) to the 3th-fourth century CE (i.e., the folded sidewalls on

the SW side of the *Decumanus*, see Sect. 3.3 and Fig. 5E). To understand how long after the construction of the youngest deformed man-made structures the earthquake occurred, attention was paid to potential ground shaking related effects and to post-seismic urban remodeling. Archeological explorations throughout the site, particularly at *Insula* IX (see Fig. 4B for location), unhearted traces of collapsed structures. Here, a dry masonry jamb, originally part of a building serving the *Lilybaeum* sewage system (Fig. 10A), collapsed in a domino-like pattern with masonry blocks falling toward the N75E direction almost orthogonal to the coseismic deformation front (see inset 1in Fig. 10A). Directional, domino-arranged building collapses are typically associated with seismic destruction (Stiros 1996). Archaeologists (Baumer and Mistretta 2020), found the collapsed feature sealed by a soil layer containing several coins and a bronze steelyard (Fig. 10B left-panel).A numismatic study performed on the two better-preserved coins (courtesy of Prof. G. Guzzetta), revealed that they were minted between the 350 and 361 CE, as they belong to the series with the legend FEL TEMP REPARATIO (see Carson et al. 1960, Plate II, Fig. 2295 for comparison, Fig. 10B right-panel).

Age constraints from the soil layer predating the collapse allow us to assert that the seismic event reasonably took place during the second half of the fourth century CE, assuming a few decades of circulation of the coins after their minting. This finding is in line with the structural transformations that occurred in the city of *Lilybaeum* after the fourth century CE, particularly in the sectors facing the *Decumanus Maximus* (see Sect. 3.2 and Palazzo and Vecchio 2013; Caruso 2008).

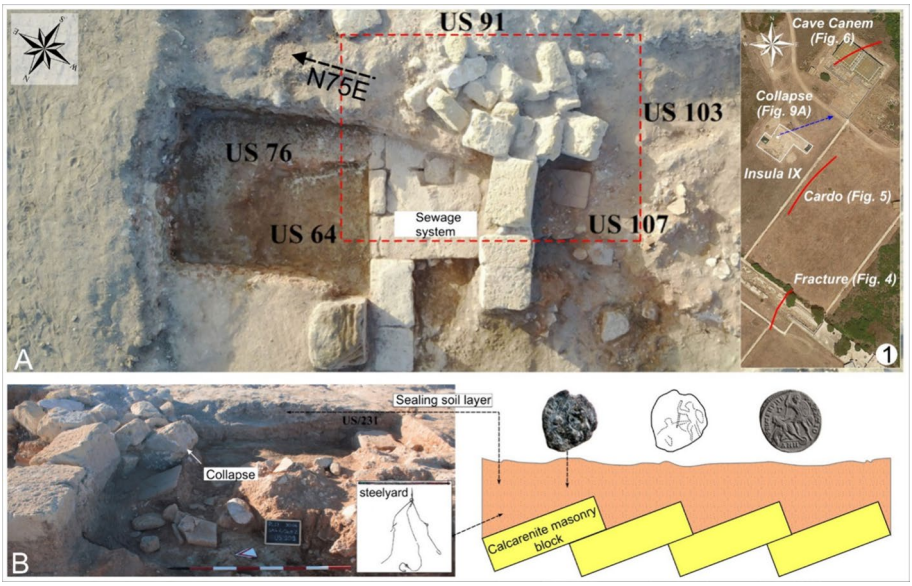

Fig. 10 **A** Aerial view of a directional (see inset 1 where red line are the trend of deformation) domino-like collapse involving a dry masonry jamb originally part of a building serving the *Lilybaeum* sewage system (courtesy of A. Mistretta, dashed blue arrow). **B** According to previous archeological studies (Baumer and Mistretta 2020), the collapse was covered by a soil-layer (left-panel) containing a number of coins and a bronze steelyard (right-panel). Ad hoc numismatic study revealed that coins were minted between the 350 and 361 CE. Age constraints from the soil layer pre-dating the collapse allow hence to assert that the seismic event reasonably took place during the second half of the fourth century CE

6 Conclusion

Archaeoseismic analysis from the ancient settlement of *Lilybaeum* in Western Sicily reveals significant deformation of archaeological remains throughout the investigated sector. Direct field observations corroborated by high-resolution aerial photogrammetry allowed for the characterization of the deformation affecting the archaeological remains within the site. In particular, accurate topographic profiling over the derived digital surface model (DSM), along with sub-surface geophysical imaging performed both on land and offshore, strongly support a tectonic origin of the deformation. Folded-to-displaced archaeological relics on land and coaxial seafloor offsets in the adjacent marine realm, roughly delineate a previously unmapped NE–SW trending active deformation front that fits well within the seismotectonic context of Western Sicily. Ground shaking related-effects such as the observed directional collapses with domino-like patterns (Fig. 10) along with urban remodeling documented in the archaeological record, strongly suggest that part of the deformation affecting the archaeological remains could have a coseismic origin. In this context, the dislocation and folding measured along well-dated archaeological features (the *Decumanus Maximus*) are interpreted as ground signatures of a coseismic slip that occurred along the reconstructed deformation front.

Considering: i) the amount of dislocation affecting the paved *Decumanus Maximus* (~ 10 cm, see Fig. 5), ii) age-constrained directional collapse (Fig. 10), and iii) Tthe reconstructed depth geometry of the accountable tectonic structure (Fig. 8), it is proposed that a back-verging reverse fault ruptured in the area, possibly at the end of the fourth century CE, resulting in a highly energetic (M ~ 6.5) earthquake. However, seismic catalogs do not provide evidence of such a large earthquake, suggesting that this event may be a missing piece in the historical seismic record. This finding offers new constraints that could be exploited to redefine the seismic potential and hazard of Western Sicily, a region where recurrence-time intervals for large earthquakes remain largely unknown and which is traversed by strategic gas pipeline systems.

Acknowledgements The governance of the Lilibeo-Marsala Archeological Park, particularly Dr. M.G. Griffo are kindly acknowledged for their willingness and support during the field operations. A. Mistretta and R. Giglio are warmly thanked for providing archaeological literature and for stimulating discussion. We are indebted to G. Guzzetta, former Professor of Ancient Numismatics at the University of Catania, for kindly providing age-constraints of the coins. The authors also acknowledge the use of MOVE Software Suite granted by Petroleum Experts Limited (www.petex.com). C. Musumeci from INGV-OE Catania is also thanked for computing some focal solutions of recent earthquakes added in Fig. 2. We express gratitude to M. Pagano for drone-shot images acquisition and processing. The research was entirely funded by the University of Catania in the framework of the project 'SeismoFront' (resp. G. Barreca), Grant n. 22722132176. A. Billi and an anonymous Reviewer are acknowledged for their constructivecomments that improved the quality of the original manuscript.

Author contribution Study conception and design, data collection and analysis were performed by Giovanni Barreca. The first draft of the manuscript was written by Giovanni Barreca, Fabrizio Pepe and Sabrina Grassi and all authors commented on previous versions of the manuscript. Material preparation was performed by Morreale Gabriele and Sebastiano Imposa. All authors read and approved the final manuscript.

Funding Open access funding provided by Università degli Studi di Catania within the CRUI-CARE Agreement. The research was entirely funded by the University of Catania in the framework of the project 'SeismoFront' (resp. G. Barreca), Grant n. 22722132176.

Declarations

Conflict of interest The authors declare that they have no conflict of interest and no financial interests are

directly or indirectly related to the work submitted for publication.

References

Accaino F, Catalano R, Di Marzo L et al (2011) A crustal seismic profile across Sicily. Tectonophysics 508:52–61. https://doi.org/10.1016/j.tecto.2010.07.011

Albanese C, Sulli A (2012) Backthrusts and passive roof duplexes in fold-and-thrust belts. The case of Central-Western Sicily based on seismic reflection data. Tectonophysics 514–517:180–198. https://doi.org/10.1016/j.tecto.2011.11.002

Alparone S, Cattaneo M, Ciaccio MG, et al (2023) Le attività del Gruppo Operativo SISMIKO durante la sequenza sismica nel 2020 a Salemi (Trapani, Italia)

Ambraseys NN (2006) Earthquakes and archaeology. J Archaeol Sci 33:1008–1016. https://doi.org/10.1016/j.jas.2005.11.006

Anderson H, Jackson J (1987) Active tectonics of the Adriatic. Region 91:937–983

Avellone G, Barchi MR, Catalano R et al (2010) Interference between shallow and deep-seated structures in the Sicilian fold and thrust belt, Italy. J Geol Soc London 167:109–126. https://doi.org/10.1144/0016-76492008-163

Balestra M, Corrado S, Aldega L et al (2019) 3D structural modeling and restoration of the Apennine-Maghrebian chain in Sicily: application for non-cylindrical fold-and-thrust belts. Tectonophysics 761:86–107. https://doi.org/10.1016/j.tecto.2019.04.014

Barker RD (1989) Depth of investigation of collinear symmetrical four-electrode arrays. Geophysics 54:1031–1037. https://doi.org/10.1190/1.1442728

Barreca G, Maesano FE (2012) Restraining stepover deformation superimposed on a previous fold-and-thrust-belt: A case study from the Mt. Kumeta-Rocca Busambra ridges (Western Sicily, Italy). J Geodyn 55:1–17. https://doi.org/10.1016/j.jog.2011.10.007

Barreca G, Barbano MS, Carbone S, Monaco C (2010a) Archaeological evidence for Roman-age faulting in central-northern Sicily: possible effects of coseismic deformation. Spec Pap Geol Soc Am 471:223–232. https://doi.org/10.1130/2010.2471(18)

Barreca G, Maesano FE, Carbone S (2010b) Tectonic evolution of the northern Sicanian-Southern Palermo Mountains range in Western Sicily: Insight on the exhumation of the thrust involved foreland domains. Ital J Geosci 129:429–440. https://doi.org/10.3301/IJG.2010.16

Barreca G, Bruno V, Cocorullo C et al (2014) Geodetic and geological evidence of active tectonics in south-western Sicily (Italy). J Geodyn 82:138–149. https://doi.org/10.1016/j.jog.2014.03.004

Barreca G, Scarfì L, Cannavò F et al (2016) New structural and seismological evidence and interpretation of a lithospheric-scale shear zone at the southern edge of the Ionian subduction system (central-eastern Sicily, Italy). Tectonics 35:1489–1505. https://doi.org/10.1002/2015TC004057

Barreca G, Scarfì L, Gross F et al (2019) Fault pattern and seismotectonic potential at the south-western edge of the Ionian Subduction system (southern Italy): New field and geophysical constraints. Tectonophysics 761:31–45. https://doi.org/10.1016/j.tecto.2019.04.020

Barreca G, Branca S, Corsaro RA et al (2020a) Slab detachment, mantle flow, and crustal collision in eastern Sicily (Southern italy): Implications on mount etna volcanism. Tectonics 39:1–19. https://doi.org/10.1029/2020TC006188

Barreca G, Bruno V, Dardanelli G et al (2020b) ¨An integrated geodetic and InSAR technique for the monitoring and detection of active faulting in southwestern Sicily. Ann Geophys. https://doi.org/10.4401/ag-8327

Barreca G, Gross F, Scarfì L et al (2021) The Strait of Messina: Seismotectonics and the source of the 1908 earthquake. Earth-Sci Rev 218:103685. https://doi.org/10.1016/j.earscirev.2021.103685

Baumer L, Mistretta A (2020) Topografia ed urbanistica di Lilibeo. Nuovi dati dagli Scavi dell'Insula IX di Capo Boeo. Antike Kunst 63:135–152

Bello M, Franchino A, Merlini S (2000) Structural model of eastern Sicily. Mem Della Soc Geol Ital 55:61–70
Ben-Avraham Z, Boccaletti M, Cello G et al (1990) Principali domini strutturali originatisi dalla collisione nogenicoquaternaria nel Mediterraneo centrale. Mem Della Soc Geol Ital 45:453–462
Bianchi F, Carbone S, Grasso M et al (1987) Sicilia orientale: profilo geologico Nebrodi – Iblei. Mem Della Soc Geol Ital 38:429–458
Billi A, Presti D, Faccenna C et al (2007) Seismotectonics of the Nubia plate compressive margin in the south Tyrrhenian region, Italy: Clues for subduction inception. J Geophys Res Solid Earth. https://doi.org/10.1029/2006JB004837
Billi A, Faccenna C, Bellier O et al (2011) Recent tectonic reorganization of the Nubia-Eurasia convergent boundary heading for the closure of the western Mediterranean. Bull La Soc Geol Fr 182:279–303. https://doi.org/10.2113/gssgfbull.182.4.279
Boschi E, Guidoboni E, Ferrari G et al (2000) Catalogue of strong Italian earthquakes from 461 a.C. to 1997. Ann Geophys 43:609–868
Carson RAG, Hill PV, Kent JPG (1960) Late Roman Bronze Coinage, A.D. 324–346, London
Caruso E (2008) Lilibeo punica e romana: storia e topografia. In: Lilibeo e il suo territorio. Contributi del Centro Internazioneale di Studi Fenici, Punici e Romani per l'archeologia marsalese. pp 73–92
Catalano R, D'Argenio B (1978) An essay of palinspastic restoration across Western Sicily. Geol Rom 17:145–159
Catalano R, D'Argenio B (1982) Schema geologico della Sicilia. Mem Della Soc Geol Ital 24:9–41
Catalano R, Di Stefano P, Sulli A, Vitale FP (1996) Paleogeography and structure of the central Mediterranean: Sicily and its offshore area. Tectonophysics 260:291–323. https://doi.org/10.1016/0040-1951(95)00196-4
Catalano R, Franchino A, Merlini S, Sulli A (2000) Central Western Sicily structural setting interpreted from seismic reflection profiles. Mem Della Soc Geol Ital 55:5–16
Catalano R, Merlini S, Sulli A (2002) The structure of Western Sicily, central Mediterranean. Pet Geosci 8:7–18
Catalano R, Valenti V, Albanese C et al (2013) Sicily's fold-thrust belt and slab roll-back: The SI.RI.PRO. seismic crustal transect. J Geol Soc London 170:451–464. https://doi.org/10.1144/jgs2012-099
Catalano R, Di Maggio C, Agate M, et al (2017) Carta geologica d'Italia alla scala 1: 50.000 e Note Illustrative del foglio 605 "Paceco." 1–232
Cinti FR, Alfonsi L, D'Alessio A et al (2015) Faulting and ancient earthquakes at Sybaris archaeological site, Ionian Calabria, Southern Italy. Seismol Res Lett 86:245–254. https://doi.org/10.1785/0220140107
D'Angelo U, Vernuccio S (1992) Carta Geologica del Foglio 617 "Marsala". Università di Palermo - Dipartimento di Geologia e Geodesia.
Dewey JF, Helman ML, Knott S et al (1989) Kinematics of the western Mediterranean. Geol Soc London, Spec Publ 45:265–283. https://doi.org/10.1144/GSL.SP.1989.045.01.1
DISS Working Group (2021) Database of Individual Seismogenic Sources (DISS), version 3.3.0: A compilation of potential sources for earthquakes larger than M 5.5 in Italy and surrounding areas
Di Stefano CA, Moscati S (1993) Lilibeo punica. Libreria dello Stato
Evans AJ (1928) The Palace of Minos at Knossos II: London, Macmillan. 547 p
Faccenna C, Becker TW, Lucente FP et al (2001a) History of subduction and back-arc extension in the central Mediterranean. Geophys J Int 145:809–820. https://doi.org/10.1046/j.0956-540X.2001.01435.x
Faccenna C, Funiciello F, Giardini D, Lucente P (2001b) Episodic back-arc extension during restricted mantle convection in the Central Mediterranean. Earth Planet Sci Lett 187:105–116. https://doi.org/10.1016/S0012-821X(01)00280-1
Faccenna C, Piromallo C, Crespo-Blanc A et al (2004) Lateral slab deformation and the origin of the western Mediterranean arcs. Tectonics. https://doi.org/10.1029/2002TC001488
Ferranti L, Oldow JS, D'Argenio B et al (2008) Active deformation in southern Italy, Sicily and southern Sardinia from GPS velocities of the peri-tyrrhenian geodetic array (PTGA). Boll Della Soc Geol Ital 127:299–316
Ferranti L, Pepe F, Barreca G et al (2019) Multi-temporal tectonic evolution of Capo Granitola and Sciacca foreland transcurrent faults (Sicily channel). Tectonophysics 765:187–204. https://doi.org/10.1016/j.tecto.2019.05.002
Ferranti L, Burrato P, Sechi D et al (2021) Late Quaternary coastal uplift of southwestern Sicily, central Mediterranean sea. Quat Sci Rev. https://doi.org/10.1016/j.quascirev.2021.106812
Finetti I., Lentini F, Carbone S, et al (2005) Geological outline of Sicily and Lithospheric Tectonodynamics of its Tyrrhenian Margin from new CROP seismic data. In: CROP PROJECT: Deep seismic exploration of the Central Mediterraneanand Italy. Elsevier, Amsterdam

Galadini F, Galli P (1999) Palaeoseismology related to the displaced Roman archaeological remains at Egna (Adige Valley, northern Italy). Tectonophysics 308:171–191. https://doi.org/10.1016/S0040-1951(99)00080-3

Galli P, Galadini F (2001) Surface faulting or archaeological relics. A review of case histories from the Dead Sea to the Alps. Tectonophysics 335:291–312. https://doi.org/10.1016/S0040-1951(01)00109-3

Gambino S, Barreca G, Gross F et al (2021) Deformation pattern of the northern sector of the malta escarpment (Offshore SE Sicily, Italy): Fault dimension, slip prediction, and seismotectonic implications. Front Earth Sci 8:1–20. https://doi.org/10.3389/feart.2020.594176

Gasparo Morticelli M, Avellone G, Sulli A et al (2017) Mountain building in NW sicily from the superimposition of subsequent thrusting and folding events during neogene: Structural setting and tectonic evolution of the kumeta and pizzuta ridges. J Maps 13:276–290. https://doi.org/10.1080/17445647.2017.1300546

Giglio, R (2006) Nuovi dati sulla topografia e sui sistemi di fortificazione di Lilibeo. Guerra e pace in Sicilia e nel Mediterraneo (VIII–III sec. aC), 1:267–281

Giglio R (2009) Lilibeo 2004–2005: la ricerca archeologica nell'area di Capo Boeo, in Ampolo C. (ed.), Immagine e immagini della Sicilia e di altre isole del Mediterraneo antico. In: Atti delle seste giornate internazionali di studi sull'area elima e la Sicilia occidentale nel contesto mediterraneo, Erice 2006. pp 561–571

Giglio Cerniglia, Rossella in "Mare internum : archeologia e culture del Mediterraneo : Lilibeo e Marsala: due città in una. 7, 2015, Pisa : Fabrizio Serra, 2015 , 2036-5160

Grassi S, De Guidi G, Patti G et al (2022) 3D subsoil reconstruction of a mud volcano in central Sicily by means of geophysical surveys. Acta Geophys 70:1083–1102. https://doi.org/10.1007/s11600-022-00774-y

Gugliota C, Gasparo Morticeli M, Avelone G et al (2014) Middle Miocene-Early Pliocene wedge-top basins of NW Sicily (Italy): Constraints for the tectonic evolution of a "non-conventional" thrust belt, affected by transpression. J Geol Soc London 171:211–226. https://doi.org/10.1144/jgs2013-009

Guidoboni E, Muggia A, Marconi C, Boschi E (2002) A case study in archaeoseismology. The collapses of the Selinunte temples (southwestern Sicily): two earthquakes identified. Bull Seismol Soc Am 92:2961–2982. https://doi.org/10.1785/0120010286

Guidoboni E, Ferrari G, Tarabusi G et al (2019) CFTI5Med, the new release of the catalogue of strong earthquakes in Italy and in the Mediterranean area. Sci Data. https://doi.org/10.1038/s41597-019-0091-9

Gutscher MA, Dominguez S, De Lepinay BM et al (2016) Tectonic expression of an active slab tear from high-resolution seismic and bathymetric data offshore Sicily (Ionian Sea). Tectonics 35:39–54. https://doi.org/10.1002/2015TC003898

Hancock PL, Altunel E (1997) Faulted archaeological relics at Hierapolis (Pamukkale), Turkey. J Geodyn 24:21–36. https://doi.org/10.1016/S0264-3707(97)00003-3

Henriquet M, Dominguez S, Barreca G et al (2020) Structural and tectono-stratigraphic review of the Sicilian orogen and new insights from analogue modeling. Earth-Sci Rev 208:103257. https://doi.org/10.1016/j.earscirev.2020.103257

Imposa S, Barone F, Chiavetta F et al (2007) A preliminary study of the subsoil of the Roman Amphitheatre of Catania (Sicily) through integrated geophysical and stratigraphic data. Nuovo Cim Della Soc Ital Di Fis C 30:577–586. https://doi.org/10.1393/ncc/i2007-10272-4

Imposa S, Grassi S, Morreale G et al (2024) New discovery of an ancient building in Akragas (Valley of Temples, Agrigento, Italy) through the integration of geophysical surveys. J Archaeol Sci Rep. https://doi.org/10.1016/j.jasrep.2023.104368

Karcz I, Kafri U (1978) Evaluation of supposed archaeoseismic damage in Israel. J Archaeol Sci 5:237–253. https://doi.org/10.1016/0305-4403(78)90042-0

Lanciani R (1918) Segni di terremoti negli antichi edifzi di Roma antica: Roma, Bollettino della Archeologia Comunale. p. 1–30.

Lavecchia G, Ferrarini F, de Nardis R et al (2007) Active thrusting as a possible seismogenic source in Sicily (Southern Italy): some insights from integrated structural-kinematic and seismological data. Tectonophysics 445:145–167. https://doi.org/10.1016/j.tecto.2007.07.007

Lentini F, Carbone S (2014) Geologia della Sicilia—geology of Sicily

Leonard M (2010) Earthquake fault scaling: Self-consistent relating of rupture length, width, average displacement, and moment release. Bull Seismol Soc Am 100:1971–1988. https://doi.org/10.1785/0120090189

Loke MH, Acworth I, Dahlin T (2003) A comparison of smooth and blocky inversion methods in 2D electrical imaging surveys. Explor Geophys 34:182–187. https://doi.org/10.1071/EG03182

McKenzie D (1972) Active tectonics of the Mediterranean Region. Geophys J R Astron Soc 30:109–185. https://doi.org/10.1111/j.1365-246X.1972.tb02351.x
Meschis M, Scicchitano G, Roberts GP, Robertson J, Barreca G, Monaco C, et al (2020) Regional deformation and offshore crustal local faulting as combined processes to explain uplift through time constrained by investigating differentially uplifted Late Quaternary paleoshorelines: The foreland Hyblean Plateau, SE Sicily. Tectonics, 39, e2020TC006187. https://doi.org/10.1029/2020TC006187
Mistretta A (2016) Il Progetto Lilibeo. Genesi ed evoluzione di un centro punico-ellenistico nella Sicilia nord-occidentale. Antike Kunst 59:123–131
Mistretta A (2022) Zur urbanen Morphologie von Lilybaeum—Grabungen insula IX 2020–21. Antike Kunst 65:
Molin D, Bernardini F, Caracciolo C. et al (2008) Materiali per un catalogo dei terremoti italiani: revisione della sismicità minore del territorio nazionale. Quad. di Geofis.
Monaco C, Tortorici L (1995) Tectonic role of ophiolite-bearing terranes in the development of the Southern Apennines orogenic belt. Terra Nova 7:153–160. https://doi.org/10.1111/j.1365-3121.1995.tb00684.x
Monaco C, Mazzoli S, Tortorici L (1996) Active thrust tectonics in Western Sicily (southern Italy): The 1968 Belice earthquake sequence. Terra Nova 8:372–381. https://doi.org/10.1111/j.1365-3121.1996.tb00570.x
Morticelli MG, Valenti V, Catalano R et al (2015) Deep controls on foreland basin system evolution along the Sicilian fold and thrust belt. Bull La Soc Geol Fr 186:273–290. https://doi.org/10.2113/gssgfbull.186.4-5.273
Morticelli MG, Avellone G, Sulli A et al (2017) Mountain building in NW sicily from the superimposition of subsequent thrusting and folding events during neogene: Structural setting and tectonic evolution of the kumeta and pizzuta ridges. J Maps 13:276–290. https://doi.org/10.1080/17445647.2017.1300546
Neri G, Barberi G, Oliva G, Orecchio B (2005) Spatial variations of seismogenic stress orientations in Sicily, south Italy. Phys Earth Planet Inter 148:175–191. https://doi.org/10.1016/j.pepi.2004.08.009
Noller JS, Lightfoot KG (1997) An archaeoseismic approach and method for the study of active strike slip faults. Geoarchaeology 12:117–135. https://doi.org/10.1002/(SICI)1520-6548(199703)12:2%3c117::AID-GEA2%3e3.0.CO;2-7
Ogniben L (1960) Stratigraphie tectono-sedimentaire de la Sicile. Mem.h.sSocGeolFrance II:203–216
Palazzo P, Vecchio P (2013) Il Decumano Massimo di Lilibeo: Ipotesi di Periodizzazione di un Settore Urbano Della Città Antica, Epigrafia
Parrino N, Pepe F, Burrato P et al (2022) Elusive active faults in a low strain rate region (Sicily. Hints from a multidisciplinary land-to-sea approach. Tectonophysics, Italy). https://doi.org/10.1016/j.tecto.2022.229520
Patti G, Grassi S, Morreale G et al (2021) Geophysical surveys integrated with rainfall data analysis for the study of soil piping phenomena occurred in a densely urbanized area in eastern Sicily. Nat Hazards 108:2467–2492. https://doi.org/10.1007/s11069-021-04784-9
Pipitone C, Dardanelli G, Brutto M Lo, et al (2020) Use of CORS Time Series for Geodynamics Applications in Western Sicily (Italy)
Pondrelli S, Salimbeni S, Ekström G et al (2006) The Italian CMT dataset from 1977 to the present. Phys Earth Planet Inter 159:286–303. https://doi.org/10.1016/J.PEPI.2006.07.008
Ramsay JG (1967) Folding and fracturing of rocks. McGraw-Hill, New York
Rodríguez-Pascua MA, Pérez-López R, Giner-Robles JL et al (2011) A comprehensive classification of Earthquake Archaeological Effects (EAE) in archaeoseismology: application to ancient remains of Roman and Mesoamerican cultures. Quat Int 242:20–30. https://doi.org/10.1016/j.quaint.2011.04.044
Rodríguez-Pascua MÁ, Perucha MÁ, Silva PG et al (2023) Archaeoseismological evidence of seismic damage at Medina Azahara (Córdoba, Spain) from the Early 11th Century. Appl Sci. https://doi.org/10.3390/app13031601
Roure F, Howell DG, Müller C, Moretti I (1990) Late cenozoic subduction complex of Sicily. J Struct Geol 12:259–266. https://doi.org/10.1016/0191-8141(90)90009-N
Rovida A, Locati M, Camassi R et al (2020) The Italian earthquake catalogue CPTI15. Bull Earthq Eng 18:2953–2984. https://doi.org/10.1007/s10518-020-00818-y
Scarfì L, Barberi G, Barreca G et al (2018) Slab narrowing in the Central Mediterranean: the Calabro-Ionian subduction zone as imaged by high resolution seismic tomography. Sci Rep. https://doi.org/10.1038/s41598-018-23543-8
Scarfì L, Langer H, Messina A, Musumeci C (2021) Tectonic regimes inferred from clustering of focal mechanisms and their distribution in space: application to the central mediterranean area. J Geophys Res Solid Earth. https://doi.org/10.1029/2020JB020519

Schepis L (2017) La domus romano-imperiale di Marsala: rilievo, analisi e valorizzazione virtuale dell'Insula I di Capo Boeo. University of Salento, Italy
Sgroi T, de Nardis R, Lavecchia G (2012) Crustal structure and seismotectonics of central Sicily (southern Italy): New constraints from instrumental seismicity. Geophys J Int 189:1237–1252. https://doi.org/10.1111/j.1365-246X.2012.05392.x
Silvestrini M (2013) Nuove epigrafi da Lilibeo. In: Claudio Zaccaria (ed) L'Epigrafia dei Porti. Centro di Antichità Alto Adriatiche Casa Bertoli Aquileia, Aquileia, pp 207–226
Stiros S (1996) Identifcation of earthquakes from archaeological data: Methodology, criteria and limitations. Br Sch Athens, Fitch Lab Occas Pap 7:129–152
Stiros SC (2001) The AD 365 Cret earthquake and possible seismic clustering during the fourth to sixth centuries AD in the Eastern Mediterranean: a review of historical and archaeological data. J Struct Geol 23:545–562. https://doi.org/10.1016/S0191-8141(00)00118-8
Sulli A, Gasparo Morticelli M, Agate M, Zizzo E (2021) Active north-vergent thrusting in the northern Sicily continental margin in the frame of the quaternary evolution of the Sicilian collisional system. Tectonophysics. https://doi.org/10.1016/j.tecto.2021.228717
Tortorici L, Monaco C, Mazzoli S, Bianca M (2001) Timing and modes of deformation in the Western Sicilian thrust system, Southern Italy. J Pet Geol 24:191–211. https://doi.org/10.1111/j.1747-5457.2001.tb00667.x
Visini F, de Nardis R, Lavecchia G (2010) Rates of active compressional deformation in central Italy and Sicily: evaluation of the seismic budget. Int J Earth Sci 99:243–264. https://doi.org/10.1007/s00531-009-0473-x
Wells D, Coppermith JK (1994) New empirical relationships among magnitude, rupture length, rupture width, rupture area, and surface displacement. Bull Seismol Soc Am 84:974–1002. https://doi.org/10.1785/BSSA0840040974

Authors and Affiliations

G. Barreca[1,2,4] · F. Pepe[3] · A. Sulli[3] · G. Morreale[1] · S. Gambino[1] · M. Gasparo Morticelli[3] · S. Grassi[1] · C. Monaco[1,2,4] · S. Imposa[1]

✉ G. Barreca
giovanni.barreca@unict.it

[1] Dipartimento di Scienze Biologiche, Geologiche ed Ambientali, Università di Catania, Catania, Italy

[2] CRUST - Interuniversity Center for 3D Seismotectonic with Territorial Applications, Chieti, Italy

[3] Dipartimento di Scienze della Terra e del Mare (DiSTeM), University of Palermo, Palermo, Italy

[4] Istituto Nazionale di Geofisica e Vulcanologia, Osservatorio Etneo, Catania, Italy